RSC Advances

PAPER

Cite this: *RSC Adv.*, 2021, **11**, 24500

The modulation effect of pi–pi interactions on the electronic and photochromic properties of viologen complexes containing *N*,*N*′-bis(carboxyethyl)-4,4′-bipyridinium†

Guozheng Zhao * and Jinjian Liu *

Received 29th March 2021
Accepted 26th June 2021

DOI: 10.1039/d1ra02469h

rsc.li/rsc-advances

Two viologen complexes containing *N*,*N*′-bis(carboxyethyl)-4,4′-bipyridinium (BCEbpy) were prepared, namely $[Zn(H_2O)_6]\cdot(BCEbpy)\cdot(p\text{-}BDC)\cdot 3H_2O$ (**1**) and $[Co(H_2O)_6]\cdot(BCEbpy)\cdot(p\text{-}BDC)\cdot 3H_2O$ (**2**) (p-H_2BDC = 1,4-benzenedicarboxylic acid), and their crystal structures, photochromism, frontier molecular orbitals, Hirshfeld surfaces and 2D fingerprint plots were investigated. The modulation effects of pi–pi interactions were explored on the electronic and photochromic properties of compounds **1** and **2**. Due to the existence of photo-response viologen radicals, both complexes **1** and **2** display excellent photo-response properties in the sequence **1** < **2**. The results indicate that compound **1** exhibits intramolecular electron transfer; compound **2** exhibits both intramolecular and intermolecular electron transfer, which is mainly due to the change of electronic and steric structures caused by pi–pi interactions with a faster photo-response rate than that of compound **1**. The donor–acceptor modes, matching principles and inter/intramolecular atom–atom close contacts were illustrated by the density functional theory (DFT)-B3LYP/6-311(d,p) method.

Introduction

In 1952, Hirshberg *et al.* discovered that spiropyrans can undergo reversible color change under light irradiation, which is called photochromism, that is, photochromic phenomenon.[1] Photochromic materials are a new type of functional materials developed in recent years,[2] and play an increasingly important role in daily life, industry and military fields, which can be used to make photochromic accessories,[3] ultraviolet sensors,[4] optical storage devices,[5] recording media,[6] nonlinear optical materials[7] and so on. As the superior electron acceptors of photochromic materials, viologen compounds, defined as *N*,*N*′-bisubstituted-4,4′-bipyridinium dications, are one of the first choices for the construction of redox photochromic complexes due to the reason that they can be easily photoreduced accompanied by obvious color changes.[8] Therefore, the preparation of viologen photochromic materials is of great significance.

The introduction of the donor and acceptor in photochromic systems is crucial for the targeted preparation of photochromic materials.[9] To gain insight into the viologen compounds with high photo-response rate, two factors should be considered: donor and acceptor essential components, as well as matching degree between donor and acceptor. It is an appropriate and effective construction strategy to combine donor and acceptor in an acceptable crystalline complex.[10] This construction strategy not only avoids troublesome procedure but also provides a mode to obtain donor–acceptor complexes with various crystal structures, which may lead to multiple photo-responsive characteristics. In most cases, for the design and preparation of multi-component complexes, the functional portion of donor or acceptor component plays an irreplaceable role depending on the nature of the donor or acceptor.[11] In order to design a donor–acceptor unit with high photo-responsivity, strong donor and acceptor components are generally preferred.[12] As a widely used donor component, benzenedicarboxylic acid has become a crucial part of complex preparation due to its potential to form a molecular framework by hydrogen bonding and/or pi–pi interactions.[13] As an acceptor component, viologens with alkyl groups can serve as structural templates during the construction of complexes. It is known that the structural stacking of donor and acceptor components is the main factor influencing the electron transfer process.[14] Multiple stacking modes provide a possible way to modulate the interactions between components, which constitute the photochromic properties of photosensitive complexes.[15]

The modification of donor and acceptor provides an opportunity to investigate the matching degree, which is of vital

Key Laboratory of Magnetic Molecules, Magnetic Information Materials Ministry of Education, The School of Chemistry and Material Science, Shanxi Normal University, Linfen 041004, P. R. China. E-mail: zhaoguozheng@sxnu.edu.cn; liujj@sxnu.edu.cn

† Electronic supplementary information (ESI) available. CCDC 1911420 and 1975209. For ESI and crystallographic data in CIF or other electronic format see DOI: 10.1039/d1ra02469h

Table 1 Crystal data and structure refinement for **1** and **2**

Compound	**1**	**2**
CCDC code	1911420	1975209
Empirical formula	$C_{22}H_{34}ZnN_2O_{17}$	$C_{22}H_{34}CoN_2O_{17}$
Formula weight	663.88	657.44
Crystal size (mm)	0.4 × 0.2 × 0.2	0.5 × 0.4 × 0.1
Crystal system	Triclinic	Triclinic
Space group	$P\bar{1}$	$P\bar{1}$
a (Å)	7.6374(3)	7.6409(5)
b (Å)	14.0781(7)	14.0750(8)
c (Å)	14.1339(7)	14.1402(8)
α (°)	99.701(4)	99.6920(10)
β (°)	105.305(4)	105.4600(10)
γ (°)	99.451(4)	99.329(2)
Volume (Å^3)	1409.58(12)	1410.07(15)
Z	2	2
D_c (g cm^{-3})	1.564	1.548
F(000)	692	686
μ (mm^{-1})	1.959	0.692
R_1/wR_2, $[I \geq 2\sigma(I)]^{a,b}$	0.0498, 0.1317	0.0434, 0.1109
R_1/wR_2, [all data]	0.0527, 0.1347	0.0462, 0.1127

^{a} $R_1 = \sum||F_o| - |F_c||/\sum|F_o|$. ^{b} $wR_2 = [\sum w(F_o^2 - F_c^2)^2/\sum w(F_o^2)^2]^{1/2}$.

importance for the design and construction of novel photochromic materials.[16] In this study, two viologen complexes, namely $[Zn(H_2O)_6]\cdot(BCEbpy)\cdot(p\text{-}BDC)\cdot 3H_2O$ (**1**) and $[Co(H_2O)_6]\cdot(BCEbpy)\cdot(p\text{-}BDC)\cdot 3H_2O$ (**2**) (p-H_2BDC = 1,4-benzenedicarboxylic acid), were synthesized and the modulation effect of pi–pi interactions were illustrated on the electronic and photochromic properties of compounds **1** and **2**. The photoinduced electron transfer modes were explored based on crystal structures and frontier molecular orbitals. The results indicate that pi–pi interactions can effectively regulate the photochromic properties. In addition, different stacking and combination of functional donor and acceptor components result in different photo-responsivity.

Results and discussion

Structural description

Table 1 describes the crystal data and structure refinement of the two viologen complexes (**1** and **2**) containing BCEbpys with the same structural units but different transition metals (Zn and Co). Here, compound **1** is taken as the representative to discuss the specific details. As shown in Table 1, based on the X-ray single crystal analysis, compound **1** consists of one $[Zn(H_2O)_6]^{2+}$ cation, BCEbpy and p-BDC^{2-} anion as well as three constitution waters, which exist in a triclinic crystal system with the $P\bar{1}$ space group (Fig. 1). The octahedral environment is formed as an isolated structure, which contains one Zn(II) ion and six coordinated waters with Zn–O bond lengths of 2.0430–2.1002 Å, achieving charge balance with the planar structure of p-BDC^{2-} anion. In compound **1**, two pyridinium rings are distorted to some extent with torsion angles of 26.38° (C6–C7–C8–C9) and 26.54° (C5–C7–C8–C10). A hydrogen bond framework is formed with a large number of intermolecular O–H···O, improving the structural stability. In addition, there are numerous intramolecular hydrogen bonds (C–H···N) between carboxyethyl and the pyridinium ring from the same BCEbpy.

Photochromism

As expected, the two viologen complexes containing BCEbpy both exhibit photochromic properties, which are similar to those exhibited by other viologen compounds. Fig. 2 depicts photographs and UV-Vis spectra for **1**, **1P**, **2** and **2P**. According to Fig. 2, at room temperature, when exposed to 365 nm Hg light (175 W), the color of compound **1** changes from light yellow to dark yellow (**1P**) within 30 min, similar to the radical-related photochromic behaviors of reported BCEbpy-based complexes,[17] which was proven by the UV-vis and EPR spectra, which show the existence of free radicals in **1P**. From Fig. 2, the strong peaks at 404 and 622 nm for **1P** were identified to be due to the photochromism from **1** to **1P**. Furthermore, the remarkable characteristic band ($g = 1.9828$) in **1P** is consistent with that of photo-response viologen radicals (Fig. 4).[18] Besides, PXRD shows that the structure of **1** is the same as that of **1P**, which excludes the possibility of photolysis and structural transformation (Fig. 3). Therefore, due to the existence of free radicals in **1P**, the photochromic property of **1** can be ascribed to the photo-response electron transfer. **1P** is decolored in dark (48 h), and changes to dark yellow again

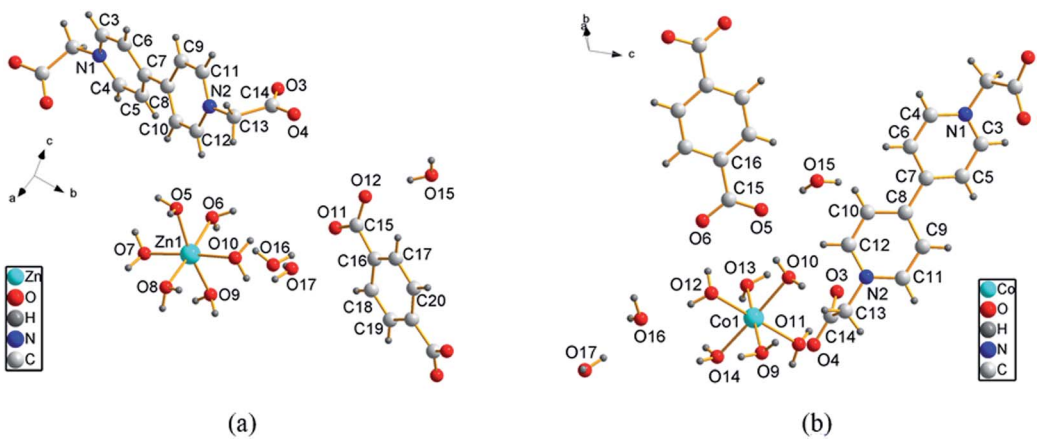

Fig. 1 Structures and atomic numbers for compounds **1** (a) and **2** (b).

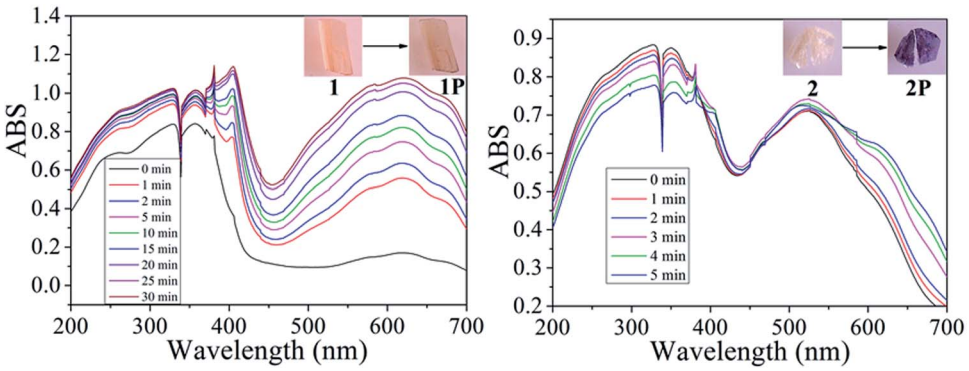

Fig. 2 Photographs and UV-Vis spectra for **1**, **1P**, **2** and **2P**.

when exposed to 365 nm Hg light at room temperature in air, repeated at least 5 times, which indicates reversible photochromism.

Compound **2** shows similar photochromic property, displaying color changes, when exposed to 365 nm Hg light (175 W). From Fig. 2, the color of compound **2** changes rapidly from light yellow to dark purple (**2P**) within 5 min. **2P** was decolored in the dark (24 h), and repeated for at least 7 consecutive cycles, indicating reversible photochromic behavior without any significant color loss. This indicates that the photochromic property of **1** is obviously weaker than that of **2**. As shown in Fig. 2, the strong characteristic signals at 402 and 617 nm for **2P** were identified due to the color change from **2** to **2P**. The presence of free radicals in **2P** was verified by remarkable EPR characteristic bands ($g = 1.9768$) (Fig. 4). PXRD results of compound **2** are in line with those of compound **1** (Fig. 3).

The structures of two viologen complexes containing BCEbpy were investigated to further analyze the influence of weak interactions on the photochromic properties. It is known that for viologen-based compounds the ability of electron transfer from an electron-rich group to an electron-deficient group plays an irreplaceable role in the photo-response rate.[19] The N2–O3 and N2–O4 distances between carboxyethyl and bipyridinium (intramolecule) are 2.691 and 3.602 Å (Fig. S2†), respectively, as well as the bond angles C11–N2–O3 and C11–N2–O4 are 86.44° and 108.72°, respectively, in compound **1**. The N2–O1 distance between BCEbpy and *p*-BDC^{2-} anion (intermolecule), and N2–O3 and N2–O4 distances between carboxyethyl and bipyridinium (intramolecule) are 3.956, 2.685 and 3.599 Å, respectively. The bond angles C11–N2–O1, C11–N2–O3 and C11–N2–O4 are 127.55°, 117.19° and 123.21°, respectively, in compound **2** (Fig. S2 and S3†), which are consistent with the general distance (less than 4 Å) between electron donors and acceptors.[20] This indicates that compound **1** exhibits intramolecular electron transfer, revealing that the electron deficient bipyridinium unit obtains electrons from the carboxyethyl O atoms of BCEbpy; compound **2** exhibits both intramolecular and intermolecular electron transfer with the bipyridinium units obtaining electrons from the carboxyethyl O atoms of BCEbpy and carboxylate O atoms of the *p*-BDC^{2-} anion, respectively, indicating that compound **2** changes color more easily than compound **1** to a certain degree.

Based on the photochromism results, compounds **1** and **2** exhibit the photo-response rates in the sequence **1** < **2** with the same BCEbpy, *p*-BDC^{2-} anion and bifunctional waters

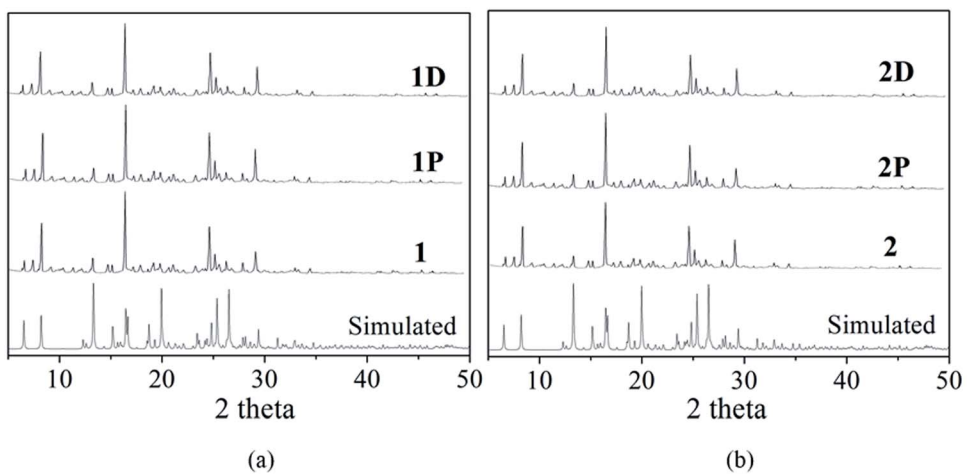

Fig. 3 PXRD of compounds **1** (a) and **2** (b).

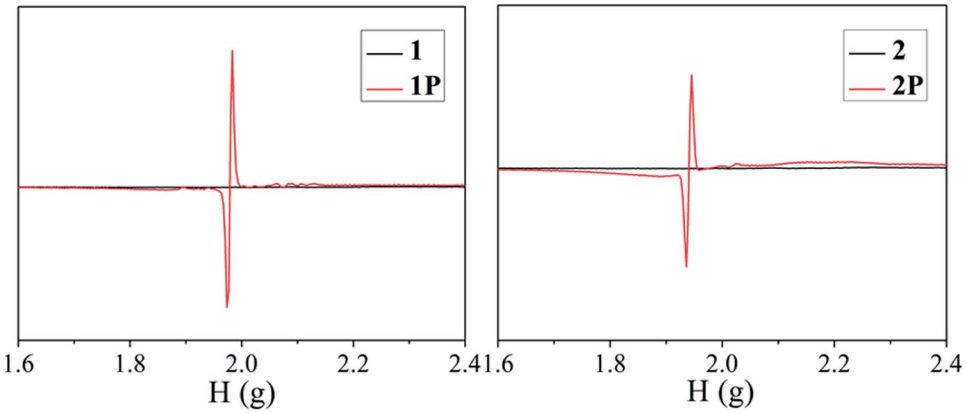

Fig. 4 EPR spectra for 1, 1P, 2 and 2P.

(constitution water and coordinated water) under the same experimental conditions. Therefore, for compounds **1** and **2**, the difference of photo-response rates mainly depends on the difference of electronic and steric structures. Fig. 5 describes the noncovalent interactions and bond paths of compounds **1** and **2** based on the density functional theory calculations. As shown in Fig. 5, according to the color-filled reduced density gradient (RDG) isosurface, different types of regions were identified by simply examining the colors. In compound **1**, between BCEbpy and *p*-BDC^{2-} anion, the green elliptical slabs show the existence of hydrogen bonds. Due to the long distance between BCEbpy and *p*-BDC^{2-} anion, there is no pi–pi interaction. Except the hydrogen bonds, face-to-face pi–pi interactions are obviously present in compound **2**, which can easily be observed between the bipyridinium rings and *p*-BDC^{2-} anion rings. The pi–pi interactions marked by green slabs in compound **2** cause the change of electronic and steric structures, and further improve the intermolecular electron transfer from O atoms of the *p*-BDC^{2-} anion to bipyridinium rings, resulting in the faster photo-response rate. In addition, the red regions in the center of the bipyridinium and *p*-BDC^{2-} anion rings depict a steric effect for compounds **1** and **2**. From Fig. S5,† for compound **2**, the rate increases rapidly in response to light stimulation and gives a constant rate, where $k_2 = 2.09 \times 10^{-3}$. For compound **1**, the reaction speed is slow due to the weak photosensitivity, showing $k_1 = 1.22 \times 10^{-4}$. Thus, it can be concluded that the photochromic speed of compound **2** is indeed faster than that of compound **1**.

Molecular orbitals

For the classic electron donor–acceptor modes of compounds **1** and **2**, the bipyridinium unit and carboxyl moiety are the electron-withdrawing and electron-donating group, respectively. Theoretical calculations were applied to gain insight into the donor–acceptor structures. Fig. 6 indicates the highest occupied molecular orbital (HOMO) and the lowest unoccupied molecular orbital (LUMO) for compounds **1** and **2**. From Fig. 6, for compound **1a**, HOMO and LUMO are mainly located on the carboxyethyl group and bipyridinium ring from the same BCEbpy, respectively, revealing that the carboxyethyl group

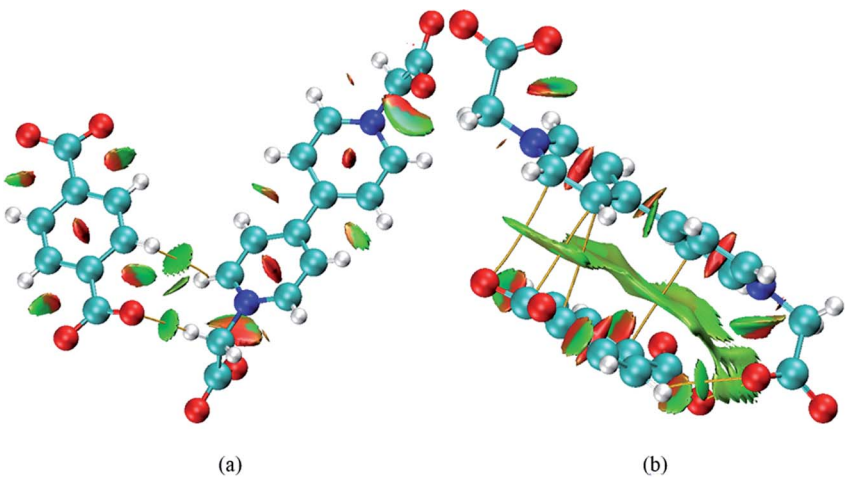

Fig. 5 Noncovalent interactions and bond paths of compounds 1 (a) and 2 (b) (blue: strong attraction; green: weak interaction; red: strong repulsion).

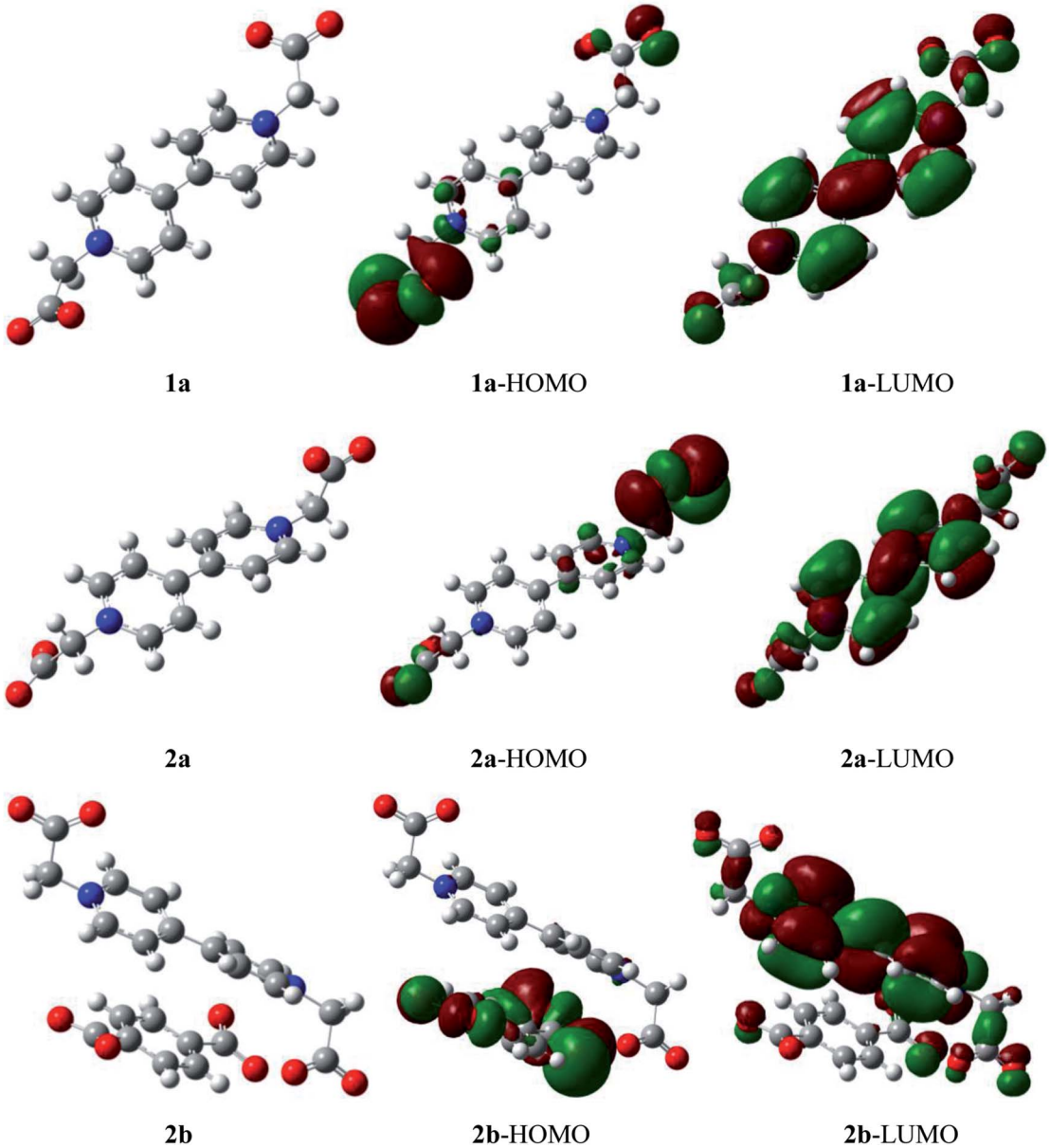

Fig. 6 Frontier molecular orbitals for compounds 1 and 2.

transfers electrons to the bipyridinium ring by HOMO–LUMO excitation, that is, intramolecular transfer. For compound **2a**, similar to **1a**, the HOMO and LUMO are mainly located on the carboxyethyl group and bipyridinium ring from BCEbpy, respectively, that is, intramolecular electron transfer; for compound **2b**, the *p*-BDC^{2-} anion and bipyridinium ring are involved in the HOMO and LUMO, respectively, illustrating that the *p*-BDC^{2-} anion transfers electrons to the bipyridinium ring by HOMO–LUMO excitation, that is, intermolecular transfer. These results are consistent with the conclusions of structural analysis.

Hirshfeld surface and 2D fingerprint plot

In order to further study the inter/intramolecular atom–atom close contacts by the fraction of intercontact, Hirshfeld surfaces and 2D fingerprint plots were examined by analyzing the types and regions of intercontacts.[21] As the input file, the experimental structures **1c** and **2c** were chosen from compounds **1** and **2**, respectively. Fig. 7 depicts the relative contributions to Hirshfeld surfaces for the close contacts. As shown in Fig. 7, for **1c**, the fractions of H···H (32.2%), O···H (25.8%), H···O (23.2%) contacts are obviously higher than those of other contacts; for **2c**, the fractions of H···H (36.2%), O···H (24.5%), H···O (21.0%) contacts are obviously higher than those of other contacts, indicating typical features in Fig. 7, which mainly consist of hydrogen bonds O–H···O from constitution water and coordinated water, improving the stability of compounds **1** and **2**. Furthermore, the fractions of atom–atom close contacts (H···H, O···H, H···O, C···H, H···C, *etc.*) of **1c** are similar with those of **2c**, indicating that the

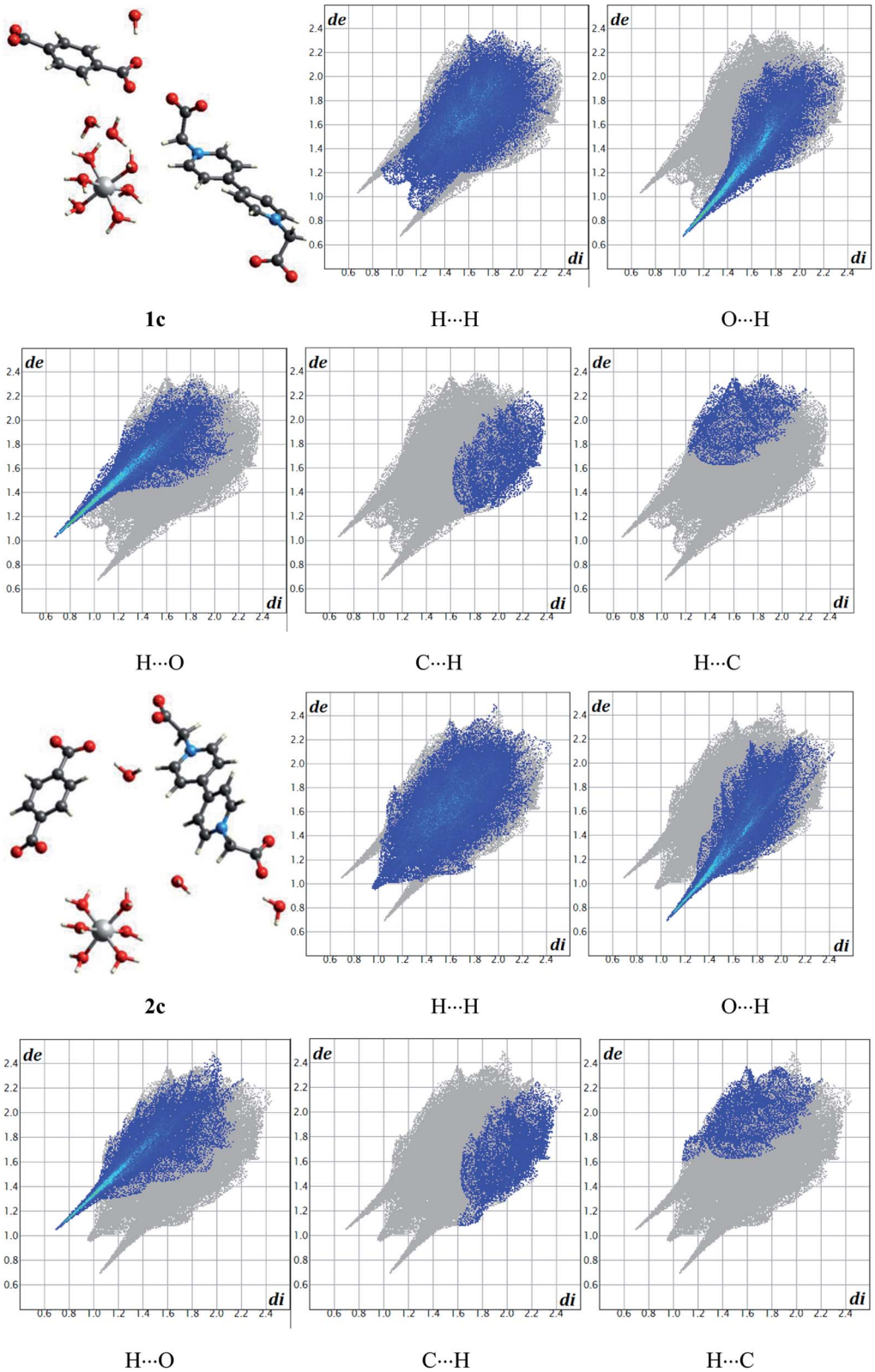

Fig. 7 Relative contributions to Hirshfeld surfaces for the close contacts of experimental structures **1c** and **2c**.

modulation effect of pi–pi interaction, rather than transition metal, is the main influencing factor on the electronic and photochromic properties of viologen complexes containing BCEbpy.

Conclusions

In this study, two viologen complexes, namely $[Zn(H_2O)_6]\cdot(BCEbpy)\cdot(p\text{-}BDC)\cdot 3H_2O$ (**1**) and $[Co(H_2O)_6]\cdot(BCEbpy)\cdot(p\text{-}BDC)\cdot 3H_2O$ (**2**) (p-H_2BDC = 1,4-benzenedicarboxylic acid), were successfully synthesized and characterized by X-ray crystallography. Compounds **1** and **2** both exist in a triclinic crystal system with the $P\bar{1}$ space group. With excellent photochromic properties, compound **1** exhibits intramolecular electron transfer from the carboxyethyl O atoms of BCEbpy to the electron deficient bipyridinium unit; compound **2** exhibits both intramolecular and intermolecular electron transfer with the bipyridinium units obtaining electrons from the carboxyethyl O atoms of BCEbpy and carboxylate O atoms of p-BDC^{2-} anion, respectively, which are in line with the results of the HOMO and LUMO analysis, revealing that compound **2** changes color more easily than compound **1**. For compound **2**, face to face pi–pi interactions between the bipyridinium rings and p-BDC^{2-} anion rings cause changes of the electronic and steric structures and further improves the intermolecular electron transfer, resulting in a much faster photo-response rate. For **1c**, the fractions of close contacts of H···H, O···H, H···O, C···H, H···C, *etc.* are similar to those of **2c**, indicating that the modulation effect of pi–pi interactions is the key influencing factor on the electronic and photochromic properties of compounds **1** and **2**.

Conflicts of interest

There are no conflicts to declare.

Acknowledgements

This work was supported by Transformation of Scientific and Technological Achievements Programs of Higher Education Institutions in Shanxi (No. 2020CG032), Linfen Key Research and Development Projects (Social Development) (No. 1909), Cultivation Plan of Young Scientific Researchers in Higher Education Institutions of Shanxi Province, Scientific and Technological Innovation Programs of Higher Education Institutions in Shanxi (No. 2019L0469), and the Fund for Shanxi "1331 Project".

Notes and references

1 Y. Hirshberg, *J. Am. Chem. Soc.*, 1956, **78**, 2304–2312.
2 (*a*) T. Lu, X. F. Yang, X. Y. Wang, Z. Y. Li, J. Yin and S. H. Liu, *Dyes Pigm.*, 2021, **185**, 108933; (*b*) J. X. Wang, C. Li and H. Tian, *Coord. Chem. Rev.*, 2021, **427**, 213579.
3 (*a*) X. T. Liu, H. L. Liu, X. G. Tang, G. Liu and S. Z. Pu, *Tetrahedron*, 2021, **78**, 131788; (*b*) Z. H. Li, L. P. Xue and Q. P. Qin, *J. Solid State Chem.*, 2021, **293**, 121755.
4 (*a*) S. X. Peng, J. F. Lv, G. Liu, C. B. Fan and S. Z. Pu, *Tetrahedron*, 2020, **76**, 131618; (*b*) Y. Z. Li, X. Y. Chen, T. Y. Weng, J. F. Yang, C. R. Zhao, B. Wu, M. Zhang, L. L. Zhu and Q. Zou, *RSC Adv.*, 2020, **10**, 42194–42199.
5 (*a*) A. Dutta, A. Singh, X. X. Wang, A. Kumar and J. Q. Liu, *CrystEngComm*, 2020, **22**, 7736–7781; (*b*) J. R. Otaegui, P. Rubirola, D. Ruiz-Molina, J. Hernando and C. Roscini, *Adv. Opt. Mater.*, 2020, **8**, 2001063.
6 Y. H. Zhan, Z. W. Yang, Z. Xu, Z. Hu, X. Bai, Y. T. Ren, M. J. Li, A. Ullah, I. Khan, J. B. Qiu, Z. G. Song, B. T. Liu and Y. H. Wang, *Chem. Eng. J.*, 2020, **394**, 124967.
7 (*a*) N. Wazzan, *Optik*, 2020, **207**, 163895; (*b*) C. Tonnele, B. Champagne, L. Muccioli and F. Castet, *Chem. Mater.*, 2019, **31**, 6759–6769.
8 (*a*) X. N. Li, L. Li, Z. H. Wang, G. H. Wu, S. Q. Liu and H. Zhang, *Dyes Pigm.*, 2021, **184**, 108800; (*b*) J. J. Shen, X. L. Kang, P. F. Hao and Y. L. Fu, *Inorg. Chem. Front.*, 2020, **7**, 4865–4871; (*c*) T. Fu, Y. L. Wei, C. Zhang, L. K. Li, X. F. Liu, H. Y. Li and S. Q. Zang, *Chem. Commun.*, 2020, **56**, 13093–13096; (*d*) Q. Sui, P. Li, R. Sun, Y. H. Fang, L. Wang, B. W. Wang, E. Q. Gao and S. Gao, *J. Phys. Chem. Lett.*, 2020, **11**, 9282–9288.
9 (*a*) G. Brunet, E. A. Suturina, G. P. C. George, J. S. Ovens, P. Richardson, C. Bucher and M. Murugesu, *Chem.–Eur. J.*, 2020, **26**, 16455–16462; (*b*) D. M. Sanchez, U. Raucci, K. N. Ferreras and T. J. Martinez, *J. Phys. Chem. Lett.*, 2020, **11**, 7901–7907.
10 (*a*) B. Verma, R. N. Baghel, D. P. Bisen, N. Brahme and A. Khare, *J. Alloys Compd.*, 2020, **838**, 155326; (*b*) P. Liesfeld, Y. Garmshausen, S. Budzak, J. Becker, A. Dallmann, D. Jacquemin and S. Hecht, *Angew. Chem., Int. Ed.*, 2020, **59**, 19352–19358; (*c*) K. Klaue, W. J. Han, P. Liesfled, F. Berger, Y. Garmshausen and S. Hecht, *J. Am. Chem. Soc.*, 2020, **142**, 11857–11864.
11 (*a*) P. Li, M. Y. Guo, L. L. Gao, X. M. Yin, S. L. Yang, R. Bu and E. Q. Gao, *Dalton Trans.*, 2020, **49**, 7488–7495; (*b*) J. M. Park, C. Y. Jung, W. D. Jang and J. Y. Jaung, *Dyes Pigm.*, 2020, **177**, 108315; (*c*) J. Zhang, Y. Zeng, H. C. Lu, X. H. Chen, X. Z. Yuan and Z. Y. Fu, *Cryst. Growth Des.*, 2020, **20**, 2617–2622; (*d*) N. Mallo, A. Tron, J. Andreasson, J. B. Harper, L. S. D. Jacob, N. D. McClenaghan, G. Jonusauskas and J. E. Beves, *Chemphotochem*, 2020, **4**, 407–412.
12 (*a*) J. J. Liu, M. H. You, M. H. Li, C. C. Huang and M. J. Lin, *CrystEngComm*, 2020, **22**, 420–424; (*b*) M. B. Nielsen, N. Ree, K. V. Mikkelsen and M. Cacciarini, *Russ. Chem. Rev.*, 2020, **89**, 573–586.
13 (*a*) P. F. Hao, H. H. Zhu, Y. Pang, J. J. Shen and Y. L. Fu, *Cryst. Growth Des.*, 2020, **20**, 345–351; (*b*) Y. Zhang, M. Li, S. L. Li and X. M. Zhang, *Acta Crystallogr., Sect. C: Struct. Chem.*, 2019, **75**, 1628.
14 (*a*) P. W. Lv, C. S. Xu, J. J. Huang, C. J. Du and F. Huang, *J. Alloys Compd.*, 2020, **844**, 155880; (*b*) K. Tahara, H. Koyama, M. Fujitsuka, K. Tokunaga, X. Le, T. Majima, J. I. Kikuch, Y. Ozawa and M. Abe, *J. Org. Chem.*, 2019, **84**, 8910–8920.
15 (*a*) M. Q. Li, L. J. Chen, Z. P. Zhang, Q. F. Luo, H. B. Yang, H. Tian and W. H. Zhu, *Chem. Sci.*, 2019, **10**, 4896–4904; (*b*) M. Q. Li, L. J. Chen, Y. S. Cai, Q. F. Luo, W. L. Li, H. B. Yang, H. Tian and W. H. Zhu, *Chem*, 2019, **5**, 634–648.

16 (*a*) N. N. Zhang, R. J. Sa, S. S. Sun, M. D. Li, M. S. Wang and G. C. Guo, *J. Mater. Chem. C*, 2019, **7**, 3100–3104; (*b*) T. Gong, Q. Sui, P. Li, X. F. Meng, L. J. Zhou, J. Q. Chen, J. H. Xu, L. Wang and E. Q. Gao, *Small*, 2019, **15**, 1803468.
17 P. X. Li, M. S. Wang, L. Z. Cai, G. E. Wang and G. C. Guo, *J. Mater. Chem. C*, 2015, **3**, 253–256.
18 T. Gong, X. Yang, J. J. Fang, Q. Sui, F. G. Xi and E. Q. Gao, *ACS Appl. Mater. Interfaces*, 2017, **9**, 5503–5512.
19 X. D. Yang, L. Sun, C. Chen, Y. J. Zhang and J. Zhang, *Dalton Trans.*, 2017, **46**, 4366–4372.
20 J. K. Sun, X. H. Jin, L. X. Cai and J. Zhang, *J. Mater. Chem.*, 2011, **21**, 17667–17672.
21 M. A. Spackman and J. J. McKinnon, *CrystEngComm*, 2002, **4**, 378–392.